Neuron
Report

Molecular Bases for the Asynchronous Activation of Sodium and Potassium Channels Required for Nerve Impulse Generation

Jérôme J. Lacroix,[1] Fabiana V. Campos,[1] Ludivine Frezza,[1] and Francisco Bezanilla[1,*]
[1]Department of Biochemistry and Molecular Biology, University of Chicago, 929 East 57th Chicago, IL 60637, USA
*Correspondence: fbezanilla@uchicago.edu
http://dx.doi.org/10.1016/j.neuron.2013.05.036

SUMMARY

Most action potentials are produced by the sequential activation of voltage-gated sodium (Nav) and potassium (Kv) channels. This is mainly achieved by the rapid conformational rearrangement of voltage-sensor (VS) modules in Nav channels, with activation kinetics up to 6-fold faster than Shaker-type Kv channels. Here, using mutagenesis and gating current measurements, we show that a 3-fold acceleration of the VS kinetics in Nav versus Shaker Kv channels is produced by the hydrophilicity of two "speed-control" residues located in the S2 and S4 segments in Nav domains I–III. An additional 2-fold acceleration of the Nav VS kinetics is provided by the coexpression of the β1 subunit, ubiquitously found in mammal tissues. This study uncovers the molecular bases responsible for the differential activation of Nav versus Kv channels, a fundamental prerequisite for the genesis of action potentials.

INTRODUCTION

To initiate most action potentials in nerves and skeletal muscles, depolarizing transmembrane fluxes of Na^+ ions carried by voltage-gated sodium (Nav) channels must precede repolarizing transmembrane fluxes of K^+ ions carried by potassium (Kv) channels (Hodgkin and Huxley, 1952). This sequential activation, a prerequisite for the genesis of the action potential, is realized because, at moderate depolarized voltages around the activation threshold, pore opening in Nav channels occurs much faster than in Kv channels (Bezanilla et al., 1970; Hodgkin and Huxley, 1952; Rojas et al., 1970).

Nav and Kv channels share a similar molecular organization of four identical subunits (Kv) or related domains (Nav) that assemble in the cell membrane to delineate a central ion conduction pore surrounded by four voltage-sensor (VS) modules. Pore opening is primarily controlled by the VS that switches from resting to active conformations in response to membrane depolarizations.

It is now well accepted that pore opening in Nav channels requires the rearrangement of only three VSs (Chanda and Bezanilla, 2002; Goldschen-Ohm et al., 2013; Hodgkin and Huxley, 1952), while pore opening in Kv channels typically requires the rearrangement of four (Smith-Maxwell et al., 1998). While this distinct feature may contribute to a slightly faster pore opening in Nav channels, it is known that the main factor underlying fast activation of Nav channels is the rapid rearrangement of their VS (Armstrong and Bezanilla, 1973; Bezanilla et al., 1982). After 60 years since the landmark work of Hodgkin and Huxley (Hodgkin and Huxley, 1952), the molecular bases for the kinetic differences between voltage sensors of Na^+ and K^+ channels remain unexplained.

Here, we show that the faster activation kinetics of voltage sensors in Nav channels relative to archetypal Shaker-type Kv channels near the activation threshold is due to (1) the presence of hydrophilic Ser or Thr residues in the S2 and S4 segment of VSs in domains I–III, which speed up 3-fold the Nav VS kinetics, and (2) the presence of the ubiquitous regulatory β1 subunit, which speeds up these kinetics an additional 2-fold.

RESULTS AND DISCUSSION

In vivo, Nav channels are associated with one or more β subunits that modulate the channel's biophysical properties. The coexpression with the ubiquitous β1 subunit was shown to moderately accelerate the rate of ionic current activation in Nav channels (Moorman et al., 1990; Zhou et al., 1991). The molecular mechanism underlying this effect remains unclear and is commonly thought to involve the stabilization of a "fast gating mode" of the channel molecule by the β1 subunits.

How does the β1 subunit accelerate pore opening in Nav channels? A possible mechanism could be a modulation of the kinetics of the rearrangements of the VS by the β1 subunits. We tested this hypothesis by measuring gating currents that directly report VS movement. Figure 1A shows gating current traces recorded in *Xenopus* oocytes using activation protocols for both muscular (Nav1.4) and neuronal (Nav1.2) Nav channels with or without coexpressed β1 subunits. In both channels, the kinetics of activating gating currents (see Figure S1 available online for a detailed fitting procedure) are accelerated approximately 2-fold in the presence of β1 subunits (Figure 1B, open versus full symbols), in good agreement with the moderate acceleration of pore opening. These results constitute evidence for a direct modulation of the VS movement in Nav channels by the β1 subunits and provide a general molecular basis to explain the modulatory role of these subunits on Nav channel function.

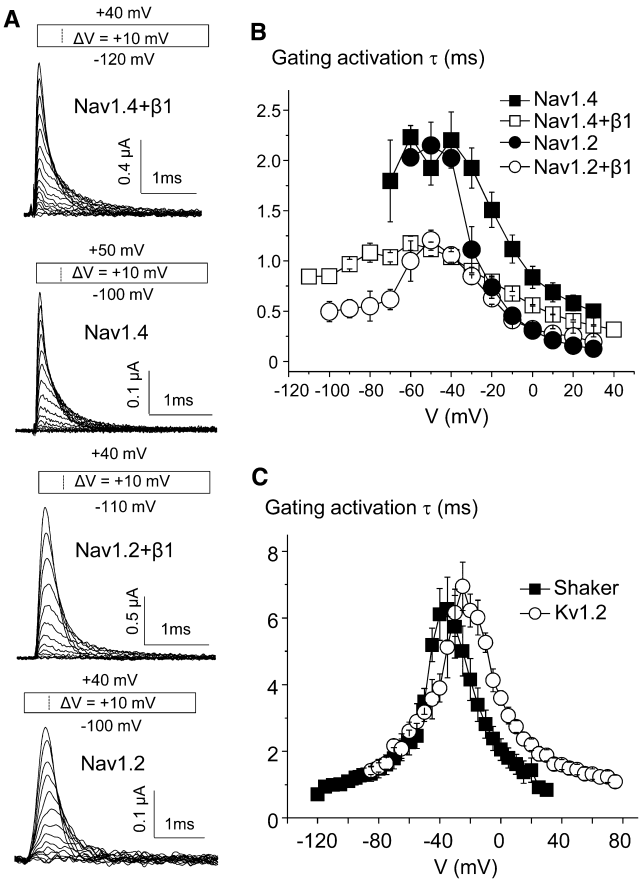

Figure 1. Acceleration of VS Movement in Mammalian Nav Channels by the β1 Subunit

(A) Activation gating current traces for Nav1.4 and Nav1.2 in presence or absence of the β1 subunit. (B) Graph showing gating current activation time constant as a function of the pulse voltage for Nav1.2 (circles) and Nav1.4 (squares) in presence (open symbols, n = 3 for Nav1.2, n = 3 for Nav1.4) or absence (full symbols, n = 4 for Nav1.2, n = 5 for Nav1.4) of the β1 subunit. (C) Graph showing the gating current activation time constant as function of the pulse voltage for Shaker (full squares) and Kv1.2 (open circles). All error bars indicate ±SEM.

The mechanism by which the β1 subunit accelerates VS kinetics in Nav channels is presently unknown to us. In the presence of the β1 subunit, the rearrangement of the VS exhibits positive cooperativity (Campos et al., 2007a; Chanda et al., 2004), which leads to accelerated VS kinetics (Chanda et al., 2004). Hence, it is tempting to speculate that the β1 subunit may act by coupling the movement of VS in adjacent domains of the Nav channel.

Yet, even in the absence of the β1 subunit, the gating currents develop up to 3-fold faster in Nav channels relative to prototypical Shaker-type Kv channels for voltages near the threshold of activation of action potentials (i.e., around −40 mV, Figures 1B and 1C). What are the molecular determinants and mechanism underlying this intrinsic kinetics difference? It is now well established that the activation of the four VSs in the α subunit of Nav channels is asynchronous: the VSs in the first three domains (DI–DIII) rearranges rapidly and controls pore opening, while the VSs in DIV rearranges with slow kinetics comparable to those of VSs found in Shaker-type Kv channels and controls fast inactivation of the sodium conductance (Chanda and Bezanilla, 2002; Goldschen-Ohm et al., 2013; Gosselin-Badaroudine et al., 2012). Hence, these observations suggest that the rapid VSs of Nav DI–DIII may possess specific molecular determinants that are absent in the slow VSs of Nav DIV and of Shaker-type Kv channels.

In order to identify such determinants, we compared the amino acid sequence of the VSs from Nav1.4 DI–DIII to the slow VSs from Nav1.4 DIV, from Shaker-type Kv channels and also from slow-activating bacterial Nav channels (Kuzmenkin et al., 2004). Two positions bear either hydrophilic residues in rapid VSs or hydrophobic residues in slow VSs. These positions are located one in the middle of the S2 segment and the other next to the outermost conserved positive residue (R1 or K1) of the S4 segment (Figure 2A). In DIII, a hydrophilic Thr is also found next to the second outermost S4-positive residue (R2). The two hydrophilic residues are not unique to Nav1.4 as they are remarkably well conserved across eukaryotic phyla (Figure S2).

To evaluate the role of these amino acids, we sought to create a "slow Nav channel" by substituting the hydrophilic residues in DI–DIII of Nav1.4 for Ile (S2) and Val (S4) (Figure 2B). Because two hydrophilic residues are present in the S4 in DIII (S4-DIII), S1120 next to K1, and T1123 next to R2 (Figures 2A and S2), we constructed three mutants: NaSlo1 (which conserves T1123), NaSlo2 (which conserves S1120), and NaSlo3 (which replaces both residues by Val). Then, we engineered a "fast Kv channel" by substituting the homologous hydrophobic residues in the slow VSs of the Shaker Kv channel (I287 in S2 and V363 in S4) by Thr. We named it Shaker-I287T/V363T (Figure 2B).

All NaSlo mutants produced a significant slowing down of the time constant of activating sodium currents (see Figure S1 for the fitting procedure) upon moderate depolarizing pulses from −45 mV to −20 mV (Figures 2C and 2D). The activation kinetics (τ) of the VS movement in the NaSlo1 and Shaker-I287T/V363T mutants were further determined using activation gating current recordings (Figure 2E) and plotted as a function of the membrane potential (Figure 2F). The τ versus voltage (V) (τ-V) curve for the NaSlo1 channel is displaced toward more negative voltages compared to the other tested channels (Figure 2F, blue triangles), presumably because the NaSlo1 mutations produce a negative shift of the charge (Q) versus V (Q-V) curve (Figure S3A, blue symbols). Nevertheless, the slowest value for the time constant of gating currents (τ_{max}) is similar between NaSlo1 and wild-type (WT) Shaker and between the Shaker-I287T/V363T and WT Nav1.4, respectively (Figures 2F and 2G). There was no statistical difference of the mean values of τ_{max} between the Shaker-I287T/V363T and WT Nav1.4 (p value = 0.32597, n = 6) and between NaSlo1 and WT Shaker (p value = 0.90888, n = 6).

Interestingly, in the NaSlo1 channel, the presence of the β1 subunit speeds up τ_{max} (about 2.5-fold) quite similarly to WT Nav1.4 channel (about 2-fold), thus suggesting that the speed-control residues do not functionally interact with the β1 subunit.

In Shaker channels, the mutations I287T-V363T also accelerate ionic current kinetics but they do so more effectively for pore closure than for pore opening (Figures S3C and S3D).

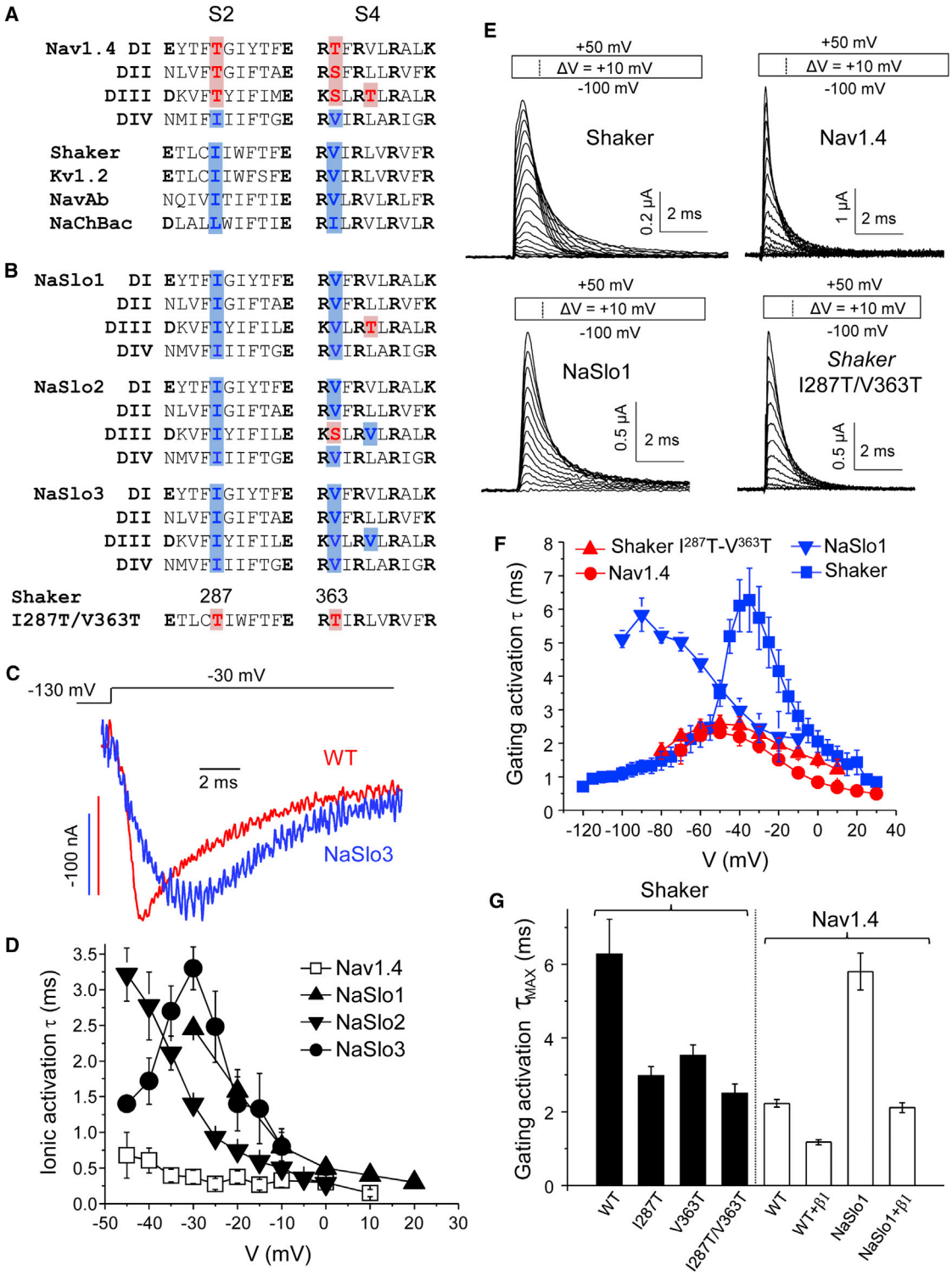

Figure 2. Two Speed-Control Residues in Voltage Sensors

(A) Portion of the S2 and S4 segments in several voltage sensors (Nav1.4, GI:116453; Shaker, GI:24642916; Kv1.2, GI:4826782; NavAB, GI:339961377; and NaChBac, GI:38489212) were aligned with respect to conserved charged residues (bold black). Rapid VSs contain hydrophilic residues at conserved speed-control sites (bold red), while slow VSs contain hydrophobic residues (bold blue) at homologous positions. (B) Sequence of the NaSlo1, Naslo2, NaSlo3, and Shaker-I287T/V363T mutants. (C) Normalized ionic current traces for WT Nav1.4 (red) and the NaSlo3 mutant (blue). (D) The time constant of the activating rise of ionic current is plotted as a function of voltage for WT (open squares, n = 4), NaSlo1 (full up triangles, n = 5), Naslo2 (full down triangles, n = 6), and Naslo3 (full

(legend continued on next page)

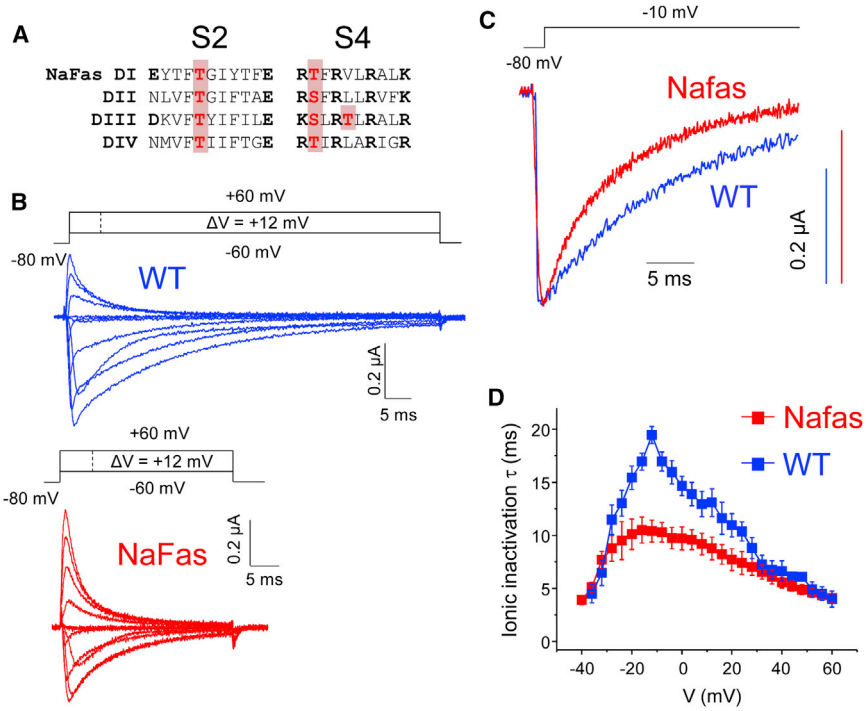

Figure 3. Hydrophilic Conversion of Speed-Control Residues in Nav1.4 DIV Accelerates Fast Inactivation

(A) Partial amino acid sequence of the NaFas mutant showing the insertion of hydroxylated Thr residues at the S2 and S4 speed-control sites in DIV. (B) Ionic current recordings for Nav1.4 WT (blue) and the NaFas mutant (red). (C) Normalized sodium current recordings for NaFas (red) and WT Nav1.4 (blue). (D) Graph showing the weighted time constant for the fast inactivation in WT Nav1.4 (blue squares, n = 5) and in the NaFas mutant (red squares, n = 7). All error bars indicate ±SEM.

This difference could be due to the fact that the I287T-V363T mutations may have little or no effect on the late concerted VS transition that rate limits pore opening (Smith-Maxwell et al., 1998) but does not rate limit pore closure (Labro et al., 2012).

If increasing the hydrophilicity of these residues accelerates the kinetics of the VS movement, then the substitution of the homologous hydrophobic residues of VS-DIV by hydrophilic amino acids should accelerate the rate of fast inactivation. The NaFas mutant was constructed by inserting Thr at the S2 and S4 sites in DIV of Nav1.4 (Figure 3A). Figures 3B–3D show that, for moderate depolarizations between −20 mV and 0 mV, the rate of fast inactivation in the NaFas mutant is accelerated up to 2-fold compared to WT channel (see Figure S1 for the fitting procedure).

Interestingly, chimeric Kv channels harboring S3-S4 regions (“paddles”) derived from Nav channels DIV displayed slower kinetics relative to chimeras harboring paddles from DI–DIII (Bosmans et al., 2008), but the latter chimeras did not systematically display fast kinetics relative to the Kv channels used to generate the chimeras. This indicated that the S3-S4 paddles of Nav channels contain only part of the determinants responsible for the specific Nav channel kinetics. This agrees well with our findings because we have identified one critical determinant contained in the S3-S4 paddle (the residue next to R1 in S4) and another one located in the S2 segment.

The mechanism by which these “speed-control” residues control the kinetics of the VS movement was investigated in Shaker Kv channels by measuring gating currents from a library of point mutations at the positions I287 and V363. Decreasing the hydrophobicity of the side chain at position I287 decreases the τ_{max} values up to 2-fold during activation and up to 4-fold during deactivation, while it also produces a small positive shift of the half-activation voltage ($V_{1/2}$) of the Q-V curve (Figure 4A and Figure S4A). On the other hand, decreasing the hydrophobicity of the amino acid at position V363 dramatically accelerated the VS movement during activation and shifted the voltage sensitivity of the VS toward more negative voltages but did not correlatively alter the deactivation kinetics (Figure 4B and Figure S4B).

The VS kinetics negatively correlates with the hydrophobicity of the side chain present at position I287. This suggests that the hydrophobicity of the side chain at position I287 defines a rate-limiting hydrophobic barrier for the gating charge movement. In this view, decreasing the hydrophobicity of this residue is expected to lower the free energy barrier between the resting and active states, thereby speeding up both activation and deactivation (Figure 4C). This hypothesis is strongly supported by previous work showing that I287 forms a hydrophobic gasket between the internal and external solutions in the core of the voltage sensor (Campos et al., 2007b). In good agreement with this conclusion, a recent molecular model of the resting conformation of the Kv1.2 voltage sensor in an explicit membrane-solvent environment shows that the hydrophobic side chain of I287 is located at the interface between two water-accessible crevices that penetrate the voltage sensor from both sides (Figure 4D) (Vargas et al., 2011). The hydrophilic substitutions in position 287 must also have a minor stabilization of the resting relative to the active position to account for the small positive Q-V shift.

In contrast to I287, increasing the hydrophobicity of V363 stabilizes the resting versus active VS conformation. Hence, the endogenous Thr present at the homologous position in the VS

circles, n = 6). (E) Gating current recordings for Shaker (top, left), Nav1.4 (top, right), NaSlo1 (bottom, left), and Shaker-I287T/V363T (bottom, right). (F) Voltage dependence of the activation gating time constant for Nav1.4 (red circles, n = 6), Shaker (blue squares, n = 6), Shaker I287T/V363T (red triangles, n = 6), and NaSlo1 (blue triangles, n = 6). (G) Mean τ_{max} values for the indicated WT or mutant Shaker (full bars) and Nav1.4 (open bars) channels. See also Figure S2 for a larger sequence alignment of eukaryotic Nav channels. All error bars indicate ±SEM.

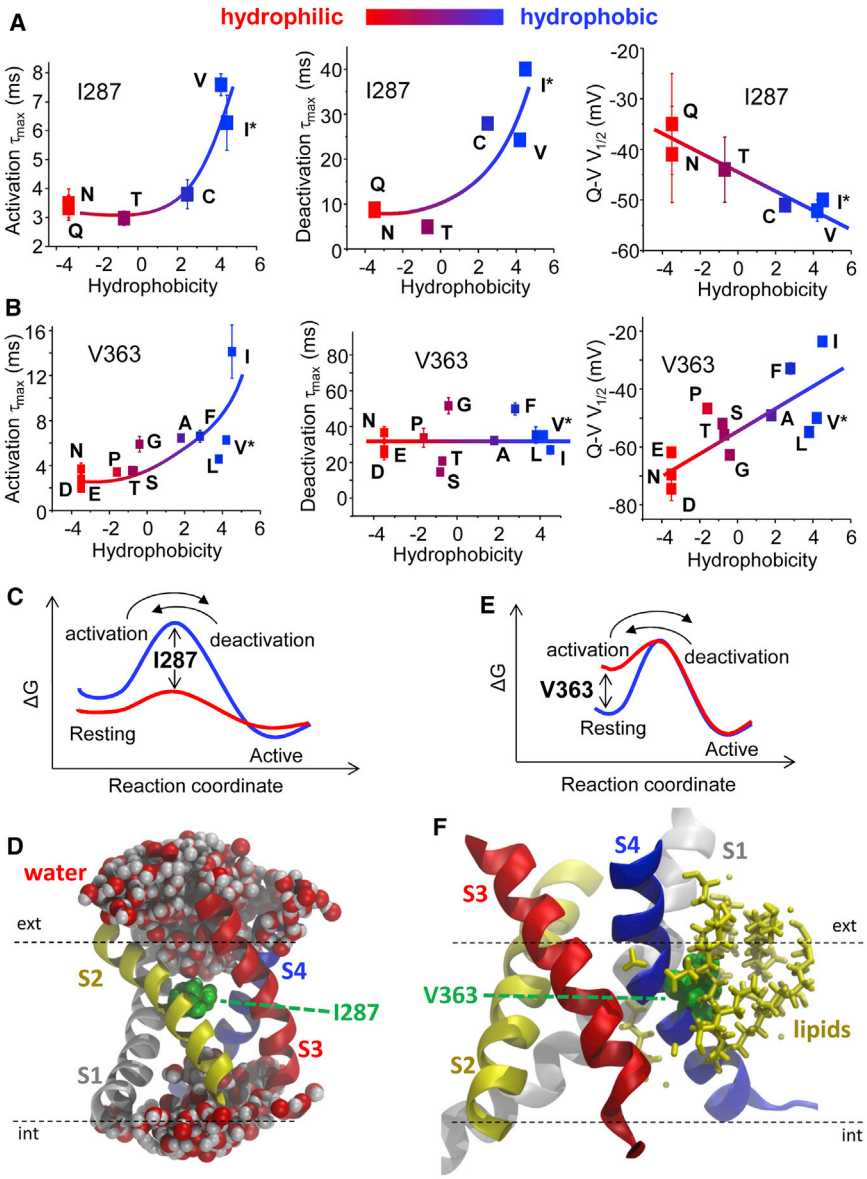

Figure 4. A Mechanism for the Speed-Control Residues in Voltage Sensors

(A and B) The $V_{1/2}$ of the Q-V curve (right) and the τ_{max} values for activation (left) and deactivation (middle) are plotted as a function of the hydrophobicity (Kyte and Doolittle, 1982) of the amino acid present at position I287 (A) and V363 (B) in the Shaker VS. The native residue is indicated by an asterisk. The data points and trend lines are gradually colored from red (more hydrophilic) to blue (more hydrophobic). The data are representative of at least five independent experiments. (C) A hypothetical two-state VS energy landscape at 0 mV helps to interpret the phenotypes for the I287 mutants: decreasing the side-chain hydrophobicity at the position of I287 (blue trace to red trace) mainly decreases the energy barrier with a small relative stabilization of the resting state. (D) The residue homologous to I287 forms a hydrophobic barrier that insulates two water-accessible pockets in a resting state model (Vargas et al., 2011). (E) Interpretation of the phenotypes for the V363 mutants using a two-state VS energy landscape at 0 mV: decreasing the side-chain hydrophobicity at the position of V363 destabilizes the resting conformation. (F) The residue homologous to V363 is surrounded by membrane lipids in a resting state model (Vargas et al., 2011). See also Figure S4 for a detailed gating current analysis of Shaker mutants. All error bars indicate ±SEM.

of Nav DI–DIII destabilizes the resting state relative to the activated state, consequently reducing the energy barrier underlying VS activation (Figure 4E). This mechanism agrees well with previous works showing that the replacement of the native residues intercalated between the Shaker S4 Arg by less hydrophobic amino acids destabilizes the resting versus the depolarized VS conformation (Xu et al., 2010). Several molecular dynamics simulations of the resting conformation of the Kv1.2 voltage sensor show that the side chain of the residue homologous to V363 points toward the lipid bilayer (Delemotte et al., 2011; Henrion et al., 2012; Jensen et al., 2010; Khalili-Araghi et al., 2010; Lacroix et al., 2012; Vargas et al., 2011). In the VS resting state, this residue is therefore probably surrounded by the hydrophobic environment of the lipid bilayer and completely buried from the solvent (Figure 4F). Hence, this VS conformation will be energetically more stable when this residue bears a hydrophobic side chain and conversely will be less stable when this side chain is made more hydrophilic (Figure 4E). Interestingly, the presence of two hydrophilic residues in S4-DIII, one after K1 and one after R2 (Figure 2A and Figure S2), may constitute the molecular basis to account for the earlier activation-onset of domain III during sodium channel activation (Chanda and Bezanilla, 2002; Gosselin-Badaroudine et al., 2012).

The mutation V363I produces the largest positive Q-V shift. Interestingly, the homologous mutation T220I in S4-DI of Nav1.5, a cardiac-specific Nav channel, is associated with early development of dilated cardiomyopathy (Olson et al., 2005). Figure S5 shows that the T220I mutation produces a positive shift of approximately +10 mV for both the channel's availability and open probability, in agreement with the V363I phenotype.

The proposed mechanism for the S4 speed-control site was further tested by conducting similar experiments in the unrelated VS from the *Ciona Intestinalis* voltage-sensitive phosphatase (Ci-VSP). Figure 5 shows that decreasing the hydrophobicity of the side chain at position L224, homologous to V363 in Shaker, negatively shifted the Q-V curve and accelerated the activation kinetics but did not significantly alter deactivation kinetics. Thus, similar mutations of this residue produce similar effects in two evolutionary-distant VSs.

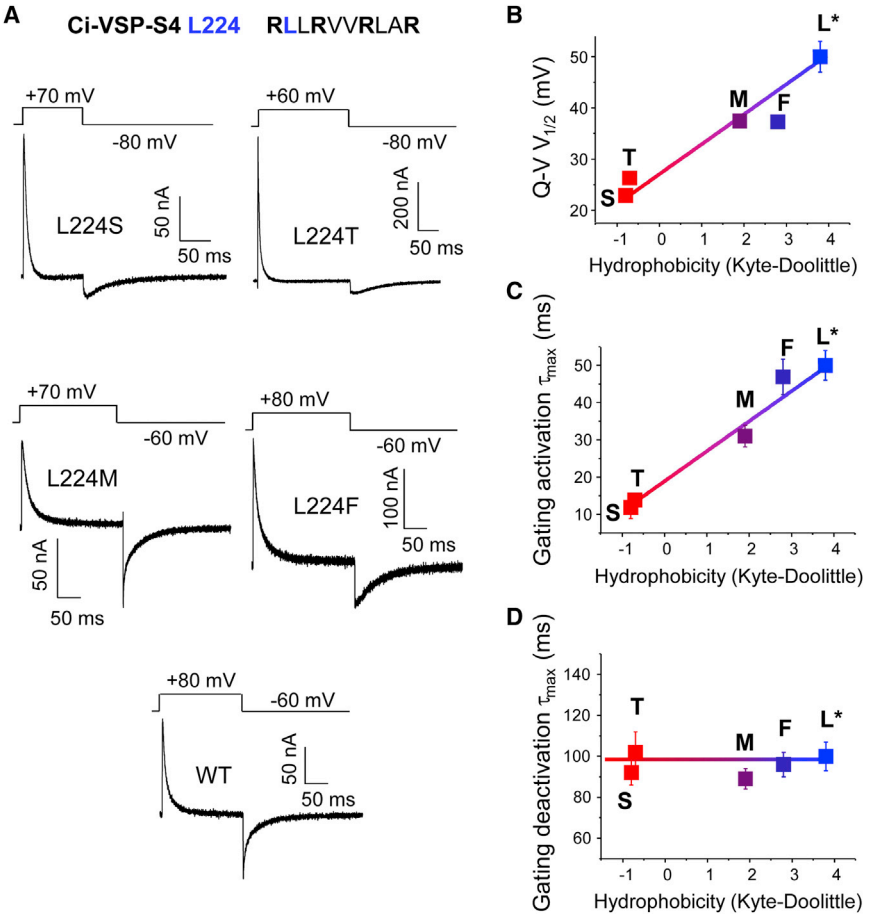

Figure 5. Gating Current Recordings for Ci-VSP L224 Mutants

(A) Activating gating current traces for the indicated L224 substitutions and WT Ci-VSP. (B–D) The plots show the relation between the $V_{1/2}$ of the Q-V curve (B), the slowest time constant (τ_{max}) recorded during activation (C) or deactivation (D), and the hydrophobicity of the side chain present at the position of L224 (Kyte-Doolittle). The trend lines and experimental points are gradually colored from red to blue according to the hydrophobicity value. The native residue L224 is indicated by an asterisk. The data in (B)–(D) are representative of four to seven independent experiments. All error bars indicate ±SEM.

From the point-of-view of evolution, it is tempting to hypothesize that the rapid VSs that characterize Nav channels were designed by natural selection during the development of nervous systems. However, this simple idea is challenged by the observation that the speed-control residues are strictly conserved in an evolutionary-distant Nav channel present in the choanoflagellate *Monosiga Brevicollis*, a unicellular eukaryotic organism (Liebeskind et al., 2011) (Figure S2). This observation suggests that, on the contrary, rapid Nav channels may have evolved prior to multicellularization, perhaps to accomplish a different task such as creating fast changes in the membrane potential. Hence, this ancient Nav channel raises the intriguing possibility that the emergence of nerve impulses may have been aided by preexisting fast Nav channels. It is then clear that the understanding of the role and function of such Nav channel ancestors will be important in delineating the evolution of nervous systems.

In summary, we show that the speed of the voltage sensors in DI–DIII of Nav channels is intrinsically accelerated by the hydrophilicity of Thr/Ser residues present at specific positions in the voltage-sensor protein. The physiological coexpression of the β1 subunit produces an additional 2-fold acceleration of the VS movement in Nav channels. A final contribution to faster activation of the sodium conductance is the fact that Nav channels conduct when only three domains are activated in contrast to Shaker-type Kv channels that require activation of all four subunits.

EXPERIMENTAL PROCEDURES

Molecular Biology and Sequence Analysis

The cDNA encoding WT Shaker channel harbors the Δ6-46 deletion that removes fast inactivation (Hoshi et al., 1990); the cDNA encoding WT Ci-VSP harbors the C363S mutation that inactivates catalytic activity (Murata et al., 2005). All mutations were introduced by Quick-Change site-directed mutagenesis (Stratagene). RNAs were produced in vitro (Ambion) and injected into *Xenopus* oocytes (50–100 ng/oocyte) 2–7 days before carrying out experiments. RNA-encoding Nav channels were injected without the rat β1 subunit unless otherwise stated.

Electrophysiology

Gating and ionic currents were recorded at room temperature (18°C) in a cut-open voltage clamp (Stefani and Bezanilla, 1998). Gating currents were measured by blocking ionic currents in Shaker with the W434F mutation (Perozo et al., 1993) and in Nav channels with 10 μM tetrodotoxin (Sigma-Aldrich) applied in the guard and external solutions. For Kv1.2 channels, the gating current time constants shown in Figure 1C were taken from a previous study (Labro et al., 2012). The composition of recording solutions for gating currents and the procedure to determine appropriate voltage pulse protocols for activation and deactivation is described elsewhere (Lacroix et al., 2012). The external solution for sodium current recordings contained 50–115 mM Na-methylsulfonate, 2 mM $CaOH_2$, 20 mM HEPES and 0–65 mM N-methylglucamine to maintain an osmolarity around 260 mOsm/l. The external Na^+ ion concentration was adjusted to maintain inward sodium currents below ~1 μA. The internal solution contained 11.5 mM Na-methylsulfonate, 104.5 mM N-methylglucamine, 2 mM EGTA, and 20 mM HEPES. For experiments with Nav1.5 and the T220I mutant, steady-state availability was determined as the relative peak current amplitude of a test pulse to −10 mV after a 300 ms prepulse to the indicated voltages.

Data Analyses

The time constant of the decaying phase of gating currents was determined using a single or double time-exponential fitting procedure (see Figure S1). A weighted time constant was calculated when a double exponential fit was used. The time constant of the activating (Nav and Kv) or deactivating (Nav) phases of ionic currents was determined using distinct monoexponential fits (see Figure S1). The $V_{1/2}$ values were determined by fitting the Q-V curves with a two-state Boltzmann function. The statistical analysis of the τ_{max} values was performed using a standard two-tailed paired Student's t test. All error bars indicate ±SEM.

SUPPLEMENTAL INFORMATION

Supplemental Information includes five figures and can be found with this article online at http://dx.doi.org/10.1016/j.neuron.2013.05.036.

ACKNOWLEDGMENTS

We thank Dr. Allan Drummond and Dr. Ramon Latorre for their insightful comments on the manuscript, Dr. Christopher Ahern and Dr. Stephan Pless for providing us with a plasmid encoding the human Nav1.5, and Dr. Ernesto Vargas for providing the pdb files for the all-atom simulation of the consensus resting state model. This work was supported by National Institutes of Health grant GM030376.

Accepted: May 25, 2013
Published: August 7, 2013

REFERENCES

Armstrong, C.M., and Bezanilla, F. (1973). Currents related to movement of the gating particles of the sodium channels. Nature *242*, 459–461.

Bezanilla, F., Rojas, E., and Taylor, R.E. (1970). Sodium and potassium conductance changes during a membrane action potential. J. Physiol. *211*, 729–751.

Bezanilla, F., White, M.M., and Taylor, R.E. (1982). Gating currents associated with potassium channel activation. Nature *296*, 657–659.

Bosmans, F., Martin-Eauclaire, M.F., and Swartz, K.J. (2008). Deconstructing voltage sensor function and pharmacology in sodium channels. Nature *456*, 202–208.

Campos, F.V., Chanda, B., Beirão, P.S., and Bezanilla, F. (2007a). beta-Scorpion toxin modifies gating transitions in all four voltage sensors of the sodium channel. J. Gen. Physiol. *130*, 257–268.

Campos, F.V., Chanda, B., Roux, B., and Bezanilla, F. (2007b). Two atomic constraints unambiguously position the S4 segment relative to S1 and S2 segments in the closed state of Shaker K channel. Proc. Natl. Acad. Sci. USA *104*, 7904–7909.

Chanda, B., and Bezanilla, F. (2002). Tracking voltage-dependent conformational changes in skeletal muscle sodium channel during activation. J. Gen. Physiol. *120*, 629–645.

Chanda, B., Asamoah, O.K., and Bezanilla, F. (2004). Coupling interactions between voltage sensors of the sodium channel as revealed by site-specific measurements. J. Gen. Physiol. *123*, 217–230.

Delemotte, L., Tarek, M., Klein, M.L., Amaral, C., and Treptow, W. (2011). Intermediate states of the Kv1.2 voltage sensor from atomistic molecular dynamics simulations. Proc. Natl. Acad. Sci. USA *108*, 6109–6114.

Goldschen-Ohm, M.P., Capes, D.L., Oelstrom, K.M., and Chanda, B. (2013). Multiple pore conformations driven by asynchronous movements of voltage sensors in a eukaryotic sodium channel. Nat Commun *4*, 1350.

Gosselin-Badaroudine, P., Delemotte, L., Moreau, A., Klein, M.L., and Chahine, M. (2012). Gating pore currents and the resting state of Nav1.4 voltage sensor domains. Proc. Natl. Acad. Sci. USA *109*, 19250–19255.

Henrion, U., Renhorn, J., Börjesson, S.I., Nelson, E.M., Schwaiger, C.S., Bjelkmar, P., Wallner, B., Lindahl, E., and Elinder, F. (2012). Tracking a complete voltage-sensor cycle with metal-ion bridges. Proc. Natl. Acad. Sci. USA *109*, 8552–8557.

Hodgkin, A.L., and Huxley, A.F. (1952). A quantitative description of membrane current and its application to conduction and excitation in nerve. J. Physiol. *117*, 500–544.

Hoshi, T., Zagotta, W.N., and Aldrich, R.W. (1990). Biophysical and molecular mechanisms of Shaker potassium channel inactivation. Science *250*, 533–538.

Jensen, M.O., Borhani, D.W., Lindorff-Larsen, K., Maragakis, P., Jogini, V., Eastwood, M.P., Dror, R.O., and Shaw, D.E. (2010). Principles of conduction and hydrophobic gating in K+ channels. Proc. Natl. Acad. Sci. USA *107*, 5833–5838.

Khalili-Araghi, F., Jogini, V., Yarov-Yarovoy, V., Tajkhorshid, E., Roux, B., and Schulten, K. (2010). Calculation of the gating charge for the Kv1.2 voltage-activated potassium channel. Biophys. J. *98*, 2189–2198.

Kuzmenkin, A., Bezanilla, F., and Correa, A.M. (2004). Gating of the bacterial sodium channel, NaChBac: voltage-dependent charge movement and gating currents. J. Gen. Physiol. *124*, 349–356.

Kyte, J., and Doolittle, R.F. (1982). A simple method for displaying the hydropathic character of a protein. J. Mol. Biol. *157*, 105–132.

Labro, A.J., Lacroix, J.J., Villalba-Galea, C.A., Snyders, D.J., and Bezanilla, F. (2012). Molecular mechanism for depolarization-induced modulation of Kv channel closure. J. Gen. Physiol. *140*, 481–493.

Lacroix, J.J., Pless, S.A., Maragliano, L., Campos, F.V., Galpin, J.D., Ahern, C.A., Roux, B., and Bezanilla, F. (2012). Intermediate state trapping of a voltage sensor. J. Gen. Physiol. *140*, 635–652.

Liebeskind, B.J., Hillis, D.M., and Zakon, H.H. (2011). Evolution of sodium channels predates the origin of nervous systems in animals. Proc. Natl. Acad. Sci. USA *108*, 9154–9159.

Moorman, J.R., Kirsch, G.E., VanDongen, A.M., Joho, R.H., and Brown, A.M. (1990). Fast and slow gating of sodium channels encoded by a single mRNA. Neuron *4*, 243–252.

Murata, Y., Iwasaki, H., Sasaki, M., Inaba, K., and Okamura, Y. (2005). Phosphoinositide phosphatase activity coupled to an intrinsic voltage sensor. Nature *435*, 1239–1243.

Olson, T.M., Michels, V.V., Ballew, J.D., Reyna, S.P., Karst, M.L., Herron, K.J., Horton, S.C., Rodeheffer, R.J., and Anderson, J.L. (2005). Sodium channel mutations and susceptibility to heart failure and atrial fibrillation. JAMA *293*, 447–454.

Perozo, E., MacKinnon, R., Bezanilla, F., and Stefani, E. (1993). Gating currents from a nonconducting mutant reveal open-closed conformations in Shaker K+ channels. Neuron *11*, 353–358.

Rojas, E., Bezanilla, F., and Taylor, R.E. (1970). Demonstration of sodium and potassium conductance changes during a nerve action potential. Nature *225*, 747–748.

Smith-Maxwell, C.J., Ledwell, J.L., and Aldrich, R.W. (1998). Uncharged S4 residues and cooperativity in voltage-dependent potassium channel activation. J. Gen. Physiol. *111*, 421–439.

Stefani, E., and Bezanilla, F. (1998). Cut-open oocyte voltage-clamp technique. Methods Enzymol. *293*, 300–318.

Vargas, E., Bezanilla, F., and Roux, B. (2011). In search of a consensus model of the resting state of a voltage-sensing domain. Neuron *72*, 713–720.

Xu, Y., Ramu, Y., and Lu, Z. (2010). A shaker K+ channel with a miniature engineered voltage sensor. Cell *142*, 580–589.

Zhou, J.Y., Potts, J.F., Trimmer, J.S., Agnew, W.S., and Sigworth, F.J. (1991). Multiple gating modes and the effect of modulating factors on the microI sodium channel. Neuron *7*, 775–785.